

Connelly, A. Langeley, N. A. Matlick, N. Nelson, O. Schofield, A. E. Smith, D. Steinberg, A. C. Steiner, B. Ver Hoven, G. Campbell and the RV *Endeavor* crew for assistance with measurements and M. R. Lewis, J. J. Cullen and C. S. Yentsch for reviewing the manuscript. This work was supported by the NSF and the NERC (UK).

Received 8 June; accepted 19 November 1987.

1. Eppley, R. W. & Peterson, B. J. *Nature* **282**, 677–680 (1979).
2. Lewis, M. R., Harrison, W. G., Oakey, N. S., Herbert, D. & Platt, T. *Science* **234**, 870–873 (1986).
3. Goldman, J. C. in *Flows of Energy and Materials in Marine Ecosystems: Theory and Practice* (ed. Fasham, M. J. R.) 137–170 (Plenum, New York, 1984).
4. Jenkins, W. J. & Goldman, J. C. *J. Mar. Res.* **43**, 465–491 (1985).
5. Platt, T. & Harrison, W. G. *Nature* **318**, 55–58 (1985).
6. Strickland, J. D. H. & Parsons, T. R. *Fish Res. Bd Can. Bull.* **167**, 310.
7. Garside, C. *Mar. Chem.* **11**, 159–167 (1982).
8. Wyman, M. & Carr, N. G. *Limnol. Oceanogr.* (in the press).
9. Glover, H. E., Campbell, L. & Prézelin, B. B. *Mar. Biol.* **91**, 193–203 (1986).
10. Prézelin, B. B., Putt, M. & Glover, H. E. *Mar. Biol.* **91**, 205–217 (1986).
11. Garside, C. *Deep Sea Res.* **32**, 723–732 (1985).
12. Glover, H. E., Smith, A. E. & Shapiro, L. J. *Plank. Res.* **7**, 519–535 (1985).
13. Iturriaga, R. & Mitchell, B. G. *Mar. Ecol. Prog. Ser.* **28**, 291–297 (1986).
14. Waterbury, J. B., Watson, S. W., Valois, F. W. & Franks, D. G. in *Photosynthetic Picoplankton* (eds Platt, T. & Li, W. K. W.) *Can. Bull. Fish. aquat. Sci.* **214**, 71–120 (1986).
15. Campbell, L. & Carpenter, E. J. *Mar. Ecol. Prog. Ser.* **32**, 139–148 (1986).
16. Campbell, L. & Carpenter, E. J. *Mar. Ecol. Prog. Ser.* **33**, 121–129 (1986).
17. Klein, P. & Coste, B. *Deep Sea Res.* **31**, 21–37 (1984).
18. Knap, A., Jickells, T., Pszenny, A. & Galloway, J. *Nature* **320**, 158–160 (1986).

## Perception of shape from shading

V. S. Ramachandran

University of California, San Diego, La Jolla, California 92093, USA

The human visual system can rapidly and accurately derive the three-dimensional orientation of surfaces by using variations in image intensity alone<sup>1–5</sup>. This ability to perceive shape from shading is one of the most important yet poorly understood aspects of human vision. Here we present several findings which may help reveal computational mechanisms underlying this ability. First, we find that perception of shape from shading is a global operation which assumes that there is only one light source illuminating the entire visual image. This implies that if two identical objects are viewed simultaneously and illuminated from different angles, then we would be able to perceive three-dimensional shape accurately in only one of them at a time. Second, three-dimensional shapes that are defined exclusively by shading can provide tokens for the perception of apparent motion, suggesting that the motion mechanism is remarkably versatile in the kinds of inputs it can use. Lastly, the occluding edges which delineate an object from its background can also powerfully influence the perception of three-dimensional shape from shading.

Our first experiment shows that the derivation of shape from shading incorporates the constraint that there is only one light source illuminating all (or most) of the image. Notice that the strong sense of depth observed in Fig. 1a is derived exclusively from shading. The sign of perceived depth, however, is ambiguous for the brain has no way of knowing what the direction of illumination is. Consequently, the objects in the display can be perceived either as being convex or concave. In preliminary experiments we found that when we perceptually ‘reversed’ the sign of depth for any one object in this display then all of the other objects reversed their sign as well. This is consistent with previous reports that when certain ambiguous visual figures are viewed simultaneously the brain seems to apply a global rather than a local strategy to resolve the ambiguity<sup>6</sup>.

These findings raise an interesting question. Is the propensity to see all the objects in Fig. 1a as simultaneously convex (or simultaneously concave) based on a tendency to assign identical depth values to all the objects or is it based on a tacit assumption

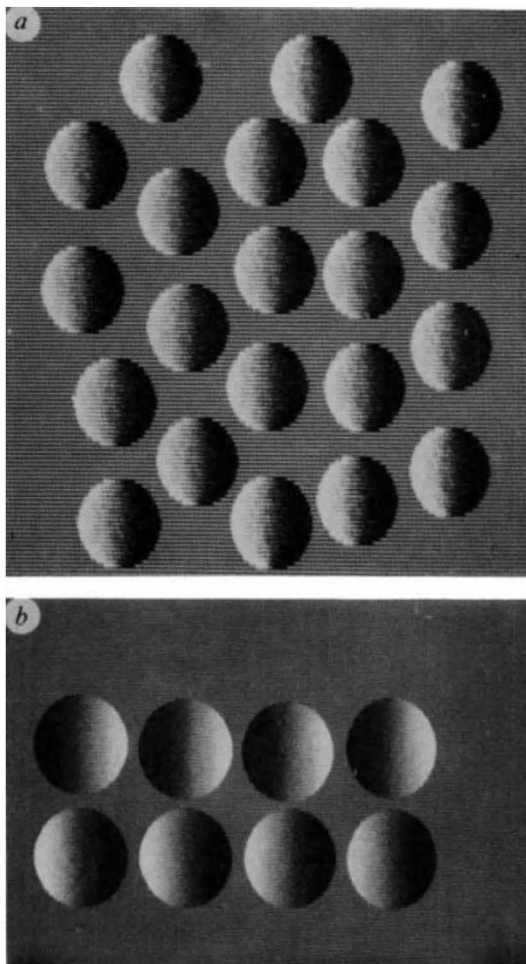
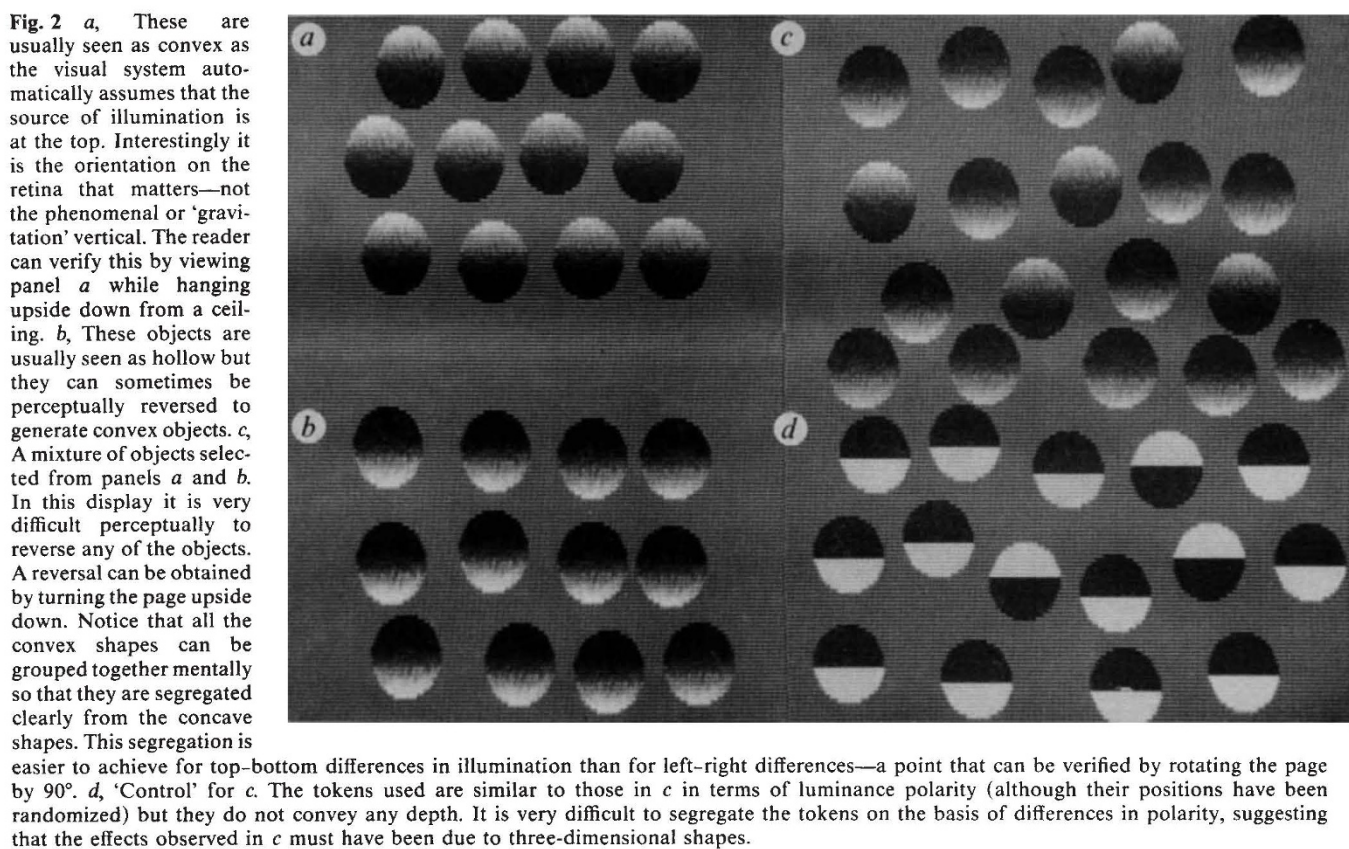


**Fig. 1** *a*, Ambiguous objects that can be seen as either spheres or holes. Depth perception in this picture can be improved by squinting one's eyes to blur the image slightly. *b*, Demonstration of the ‘single-light source’ constraint. When one horizontal row is seen as convex the other row is always seen as concave. It is very difficult to see all objects as being simultaneously convex or simultaneously concave. This simple display shows that the brain will accept only one light source at a time for the entire visual image (or large portion of it).

that there is only a single light source illuminating the image? To find out we used a display (Fig. 1b) consisting of two rows of objects which were mirror images of each other. Eleven subjects viewed this display and reported that when one row of objects was convex then the mirror images were always concave (and vice versa). It was in fact almost impossible to see all objects as being simultaneously convex or concave. Notice that either of the two horizontal rows can be seen as concave or convex when the other row is covered with a piece of cardboard. When viewed simultaneously, however, seeing one row as convex forces the visual system to see the other row as concave. This is an important observation for it suggests that the brain prefers a ‘common-light-source’ assumption to a ‘common-depth’ assumption—a principle that actually violates the Gestalt law of common fate. This may be because our brains evolved in a solar system which has only one sun. Furthermore, our observations also contradict a common misconception shared by many psychologists<sup>7</sup>—that the brain always prefers the simplest interpretation of any visual pattern. In Fig. 1b it would be simpler to see all objects as either simultaneously convex or simultaneously concave but the visual system actually rejects these interpretations.

In Fig. 2 there is a strong tendency to perceive the objects in the top left panel (*a*) as convex and those in the bottom left



panel (*b*) as concave. This suggests that in addition to the unitary-light-source constraint there is also a tendency to assume that the light source is at the top; an effect that is well known to artists. The effect is especially strong if a mixture of such objects is presented (Fig. 2*c*). In this display it is also possible to group all the convex shapes together mentally to form a cluster that is clearly segregated from the background of concave shapes. This is a surprising result as it is usually assumed that only certain elementary stimulus features such as orientation, colour and 'terminators' can be grouped together in this way<sup>8–10</sup>. Figure 2*c* shows that even three-dimensional shapes that are conveyed by shading can provide tokens for perceptual grouping and segregation. To make sure that the effect was not due to some more elementary image feature (such as luminance polarity) we produced a control stimulus (Fig. 2*d*) in which the targets were similar to those in Fig. 2*c* in terms of luminance polarity but did not convey any depth. In this display, it is difficult to segregate the tokens on the basis of differences in polarity suggesting that the effects observed in Fig. 2*c* must have been based on three-dimensional shapes. Eleven naive subjects confirmed this striking difference between the two displays when they were asked to compare them directly. Segregation is also much more pronounced for top-down differences in illumination than for left-right differences. For instance, if Fig. 2*c* is rotated by 90° perceived depth becomes less compelling and the degree of segregation is also reduced correspondingly. This further supports the view that effect depends on the three-dimensional shapes of the tokens rather than on luminance polarity.

Our next experiment shows that shapes that are defined exclusively by shading can provide an input to apparent motion. To show this we began with the two objects, a convex one, and a concave one, presented simultaneously one below the other in the first frame (Fig. 3*a*). This was switched off and replaced with the second frame in which the two objects were simply made to exchange locations (Fig. 3*b*). The frames are shown

side by side for clarity but in the original experiment they were optically superimposed and alternated rapidly. The objects were 1.5° wide and they were separated by a distance of about 2°. A very vivid impression of apparent motion could be obtained from this stimulus sequence. Eleven naive subjects reported that they could see a sphere jumping up and down as it alternatively filled and vacated two holes in the background. We varied the stimulus onset asynchrony (SOA) over a wide range, keeping the inter-stimulus interval constant at zero ms and found that apparent motion disappeared when the SOA was less than ~75 msec. Similar effects were observed when we used cylindrical targets (Fig. 3*c* and *d*) instead of circular ones. Interestingly, with cylindrical targets the depth often took 30–60 s to

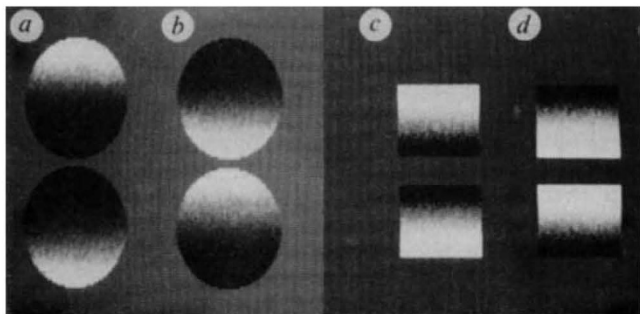


**Fig. 3** *a* and *b*, Two frames of an apparent motion sequence. In the first frame (*a*) there is a sphere on top and a 'hole' just below it. In the second frame (*b*) the two figures have exchanged places. The two frames are shown side-by-side for clarity but in the original experiment they were optically superimposed and alternated. This created the striking impression of a sphere moving vertically as it 'filled' and vacated two sockets in the background. *c* and *d* Show cylinders rather than spheres (see text). Several seconds may elapse before depth emerges in these displays.

emerge and during this long latency no apparent motion could be perceived. Once depth became clearly defined, however, the motion of the cylinder became instantly visible. We conclude that the perception of apparent motion must necessarily be preceded by a computation of three-dimensional shape from shading based on the single-light-source constraint. Certain cells in the middle temporal area of monkey cortex<sup>11</sup> are known to respond to apparent motion of texture borders<sup>12</sup> and it might be interesting to see if these cells would also respond to motion that is derived from shape perceived from shading.

Is the apparent motion seen in Fig. 3 based on shape from shading *per se* or some other more elementary image feature? It is conceivable that similarity of brightness polarity could have served as a basis for establishing correspondence in these displays. This seems unlikely as the depth impression often took 30–60 s to develop and apparent motion was never perceived until depth emerged. To show the point more directly we also used a 'control' display which conveyed no depth but was similar to Fig. 3 in terms of brightness polarity (the targets resembled the controls shown in Fig. 2d). When the two frames were alternated, random, incoherent flicker was seen and, unlike Fig. 3, there was never any impression of unambiguous vertical apparent motion. This implies that motion correspondence in Fig. 3 was being established between three-dimensional shapes rather than more primitive image features.

In deriving shape from shading the visual system can also take advantage of information provided by the occluding edges that delineate an object from its background<sup>1</sup>. We constructed Fig. 4a and b to show this principle. The luminance gradients along the horizontal axis are identical for both images (a and b) yet the surfaces look very different. Figure 4a looks like three metal cylinders touching each other, whereas Fig. 4b conveys unmistakably the impression of a corrugated metal sheet. Notice that the shape of each surface faithfully follows the contours at the upper and lower borders of the object. These contours seem to propagate inward to influence the perceived depth of the entire surfaces. Interestingly, there is also a corresponding shift in the perceived direction of illumination. In Fig. 4a the light source occupies a position exactly normal to the surface, that is, it has the same location as the observer. In Fig. 4b, on the other hand, the light seems to come from the left. It is noteworthy that such striking changes in perception can be produced simply by altering the outlines of the objects.

Even an illusory outline will produce this effect in Fig. 4c which we generated by superimposing an illusory circle<sup>13,14</sup> on a simple one-dimensional luminance gradient. This figure initially looks flat but on prolonged viewing the region corresponding to the illusory circle starts bulging out towards the observer and may even detach itself from the background to take on the appearance of a sphere. Again, this observation shows that the derivation of shape from shading can be strongly influenced by segmentation boundaries. The important role played by segmentation boundaries has also been shown by us previously for a variety of other visual capacities such as stereopsis<sup>15</sup>, apparent motion<sup>6</sup> and three-dimensional structure from motion<sup>16</sup>.

Our last experiment shows the role of top-down influences in the perception of three dimensional shape from shading. We found that when the objects were arranged in regular rows (Fig. 4d) it was sometimes possible to 'imagine' the display as a set of 16 holes in an opaque grey occluder through which we could see two cycles of a sine-wave grating<sup>17</sup>. The perceptual switch was quite compelling, and when it occurred the impression of curved three-dimensional shapes vanished completely. This shows that there is a direct and powerful interaction between occlusion cues and the derivation of shape from shading and also implies that the process can be strongly modulated by top-down influences such as visual imagery.

We find that the visual system's ability to determine the three dimensional shape of a shaded region is strongly constrained

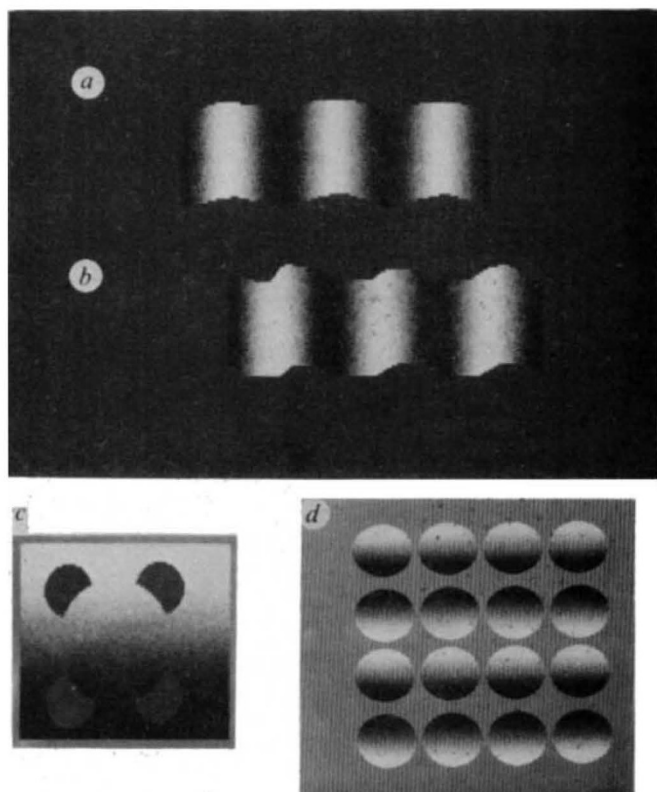


**Fig. 4** *a* and *b*, Here there are identical luminance gradients along the horizontal axis yet the surfaces look very different. In fact the surfaces seem faithfully to follow the shapes of the occluding edges at the top and bottom of each figure. The depth effect can take as long as a minute to evolve. It would help to squint your eyes slightly and to view the figures from a distance. *c*, An 'illusory' circle superimposed on a simple one-dimensional luminance gradient. The area enclosed by the circular outline bulges out to assume the appearance of a spherical object. We find this effect (as well as the 'spheres' observed in Fig. 2) can be obtained even if the luminance gradient is not a cosine function of the kind that would be associated with real spherical surfaces. *d*, This display illustrates that top-down influences can play a role in the perception of shape from shading. The display can be seen either as alternate horizontal rows of convex and concave objects or as two cycles of a sine-wave grating viewed through 16 'holes' cut out of a grey opaque occluder. The effect is easier to obtain if the page is rotated through 90°.

by the assumption that there is only one light source in the image and also by the shape of the occluding edges that delineate this area from the surround. Furthermore, once these three-dimensional shapes have been made explicit, the system can use them for a variety of visual skills such as figure-ground segregation and motion perception.

We thank Y. Fisher, D. Kleffner, D. Rogers-Ramachandran, S. Cobb, J. A. Deutsch, H. Pashler and F. H. C. Crick for their helpful comments. V. S. Ramachandran was supported by biomedical and academic senate research funds from the University of California.

*Note added in proof:* We find that only luminance-derived outlines can support the perception of three-dimensional shapes. If the object's outline is conveyed exclusively by chromatic borders, the impression of solidity disappears completely.

Received 6 August; accepted 2 November 1987.

1. Witkin, A. P. & Tenenbaum, J. M. in *Human Machine Vision* (eds Beck, J., Hope, B. & Rosenfeld, A.) 481–543 (Academic, New York, 1983).
2. Pentland, A. J. *opt. Soc. Am.* **72**, 448–455 (1982).
3. Todd, J. & Mingolla, E. *J. exp. Psychol.* **9**, 583–595 (1983).
4. Horn, B. K. P. in *The Psychology of Computer Vision* (ed. McGraw Hill, New York, 1975).
5. Yonas, A., Kuskowski, M. & Sternfels, S. *Child Dev.* **50**, 495–500 (1979).

6. Ramachandran, V. S. & Anstis, S. M. *Scient. Am.* **254**, 102–109 (1986).
7. Restle, F. in *Organization and representation in perception* (ed. Beck, J.) 31–36 (Lawrence Erlbaum, London, 1982).
8. Treisman, A. *Scient. Am.* **255**, 114–126 (1986).
9. Julesz, B. *Foundations of Cyclopean Perception* (Chicago University Press, 1971).
10. Beck, J. *Percept. Psychophys.* **1**, 300–302 (1966).
11. Albright, T. *Soc. Neurosci. Abstr.* **13**, 1626 (1987).
12. Ramachandran, V. S., Rao, V. M. & Vidyasagar, T. R. *Vision Res.* **13**, 1399–1401 (1973).
13. Gregory, R. L. *Nature* **238**, 51–52 (1972).
14. Kanizsa, G. *Scient. Am.* **234**, 48–52 (1976).
15. Ramachandran, V. S. *Percept. Psychophys.* **39**, 361–373 (1986).
16. Ramachandran, V. S., Cobb, S. & Rogers-Ramachandran, D. *Soc. Neurosci. Abstr.* **13**, 630 (1987).
17. Campbell, F. W. & Robson, J. G. *J. Physiol. Lond.* **197**, 551–556 (1968).

## Real-time imaging of evoked activity in local circuits of the salamander olfactory bulb

John S. Kauer

Departments of Neurosurgery, and Anatomy and Cell Biology,  
New England Medical Center and Tufts Medical School,  
Boston, Massachusetts 02111, USA

The encoding of olfactory information in the central nervous system (CNS) depends on spatially distributed patterns of activity generated simultaneously in many neuronal circuits<sup>1–4</sup>. Optical neurophysiological recording permits analysis of neural activity non-invasively and with high spatial and temporal resolution<sup>5</sup>. Here, a video method for imaging voltage-sensitive dye fluorescence *in vivo* is used to map neuronal activity in local circuits of the salamander olfactory bulb. The method permits the imaging of simultaneous ensemble transmembrane activity in real time. After electrical stimulation of the olfactory nerve, activity spreads centripetally from the sites of synaptic input to generate non-homogeneous response patterns that are presumably mediated by local circuits within the bulbar layers. The results also show the overlapping temporal sequences of activation of cell groups in each layer. The method thus provides high resolution, sequential video images of the spatial and temporal progression of transmembrane events in neuronal circuits after afferent stimulation and offers the opportunity for studying ensemble events in other brain regions.

The design of the recording equipment and the planar laminae of the salamander olfactory bulb are shown in Fig. 1a and b. These layers are oriented approximately perpendicular to the dorsal bulbar surface, in contrast to the concentric organization in the mammal, and can be identified by sequential recording of electrically-evoked field potentials<sup>6</sup>, characteristic of each layer, across the dorsal surface.

A highly simplified scheme of the synaptic organization of the bulb is shown in Figs 1b and 3a. Mitral/tufted and periglomerular cells receive excitatory input from afferent receptor axons. There are reciprocal dendrodendritic synapses between excitatory mitral/tufted and inhibitory periglomerular cells, and between mitral/tufted and inhibitory granule cells<sup>7</sup>. The connectivity among these widespread negative-feedback circuits, is thought to mediate the long-lasting periods of inhibition seen with electrical and odour stimulation. Electrophysiological<sup>4,8–12</sup> and 2-deoxyglucose<sup>13</sup> analyses have shown that stimulation with an odorant gives rise to spatially and temporally non-uniform patterns of activity, presumably shaped by these local bulbar circuits<sup>9,14</sup>.

To characterize these ensemble response patterns, changes in the fluorescence of the voltage-sensitive dye RH414 (ref. 15) were observed at video rates. This allowed the study of bulbar responses elicited by electrical shocks, taking advantage of the more synchronous activation these stimuli provide over odorant pulses<sup>16</sup>. The tiger salamander (*Ambystoma tigrinum*) is a useful animal<sup>8</sup> for these studies as electrophysiological recordings have

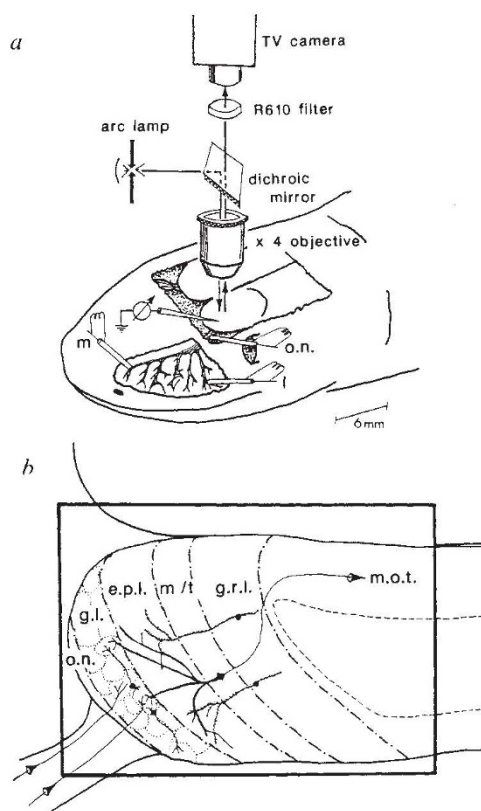


**Fig. 1** The design of the dye-recording equipment showing light source, dichroic mirror, microscope objective, filter, video camera and recording and stimulating electrodes (m, medial; l, lateral; o.n., olfactory nerve). **b**, Dorsal view of the olfactory bulb laminae schematically showing the organization of the major cell types (g.l., glomerular; e.p.l., external plexiform; m/t, mitral/tufted cell body; g.r.l., granule-cell body layers; m.o.t., medial olfactory tract). **Methods.** The animal and the electrodes were held on the stage of an Olympus BHS-2 microscope. The brain was epi-illuminated by a Kratos Analytical Instruments (Ramsey, New Jersey) 150 W xenon-mercury arc lamp with a feedback-stabilized power supply. A dichroic mirror reflected wavelengths below 580 nm, exciting RH414 ( $E_{max} = 530$  nm), and transmitted fluorescence at 610 nm through an Olympus R610 nm filter to a Dage-MTI (Michigan City, Illinois), series-68 television camera with a Newvicon tube. Sequences of 16 video frames taken at 30 frames  $s^{-1}$  (128 pixels  $\times$  128 pixels  $\times$  8 bits) were digitized and processed by an Imaging Technology (Woburn, Massachusetts) FG100-AT board in a Compaq 286 Deskpro computer (Houston, Texas). Thirty-eight land-phase animals were anaesthetized with ketamine HCl (10 mg per 100 g administered every 45–60 min), immobilized with *d*-tubocurarine (0.7 mg per 100 g), and locally anaesthetized with lidocaine at the wound and head fixation points. The voltage-sensitive dye RH414 (ref. 15) (1.5 mg ml $^{-1}$  amphibian Ringer) was placed on the exposed bulb for 20–25 min; excess dye was washed off with Ringer solution. No other voltage-sensitive dyes were tested. There was no obvious deterioration in the fluorescence or electrical signals during the 4–6 h experiments. Electrical stimulation (700  $\mu$ s duration, 2–5  $\times$  threshold) was carried out by a concentric bipolar electrode placed on the trunk of the olfactory nerve at its entry to the olfactory bulb or on dorso-lateral or dorso-medial fascicles overlying the nasal sac (see Fig. 1a). Field potentials were recorded on the surface of the bulb (see Fig. 3b). The video field shown in the frames of Fig. 2 is delineated by heavy black lines in Fig. 1b.

been made from single receptor<sup>17</sup> and bulbar<sup>8,9</sup> cells, and voltage-sensitive dye signals have been recorded with a diode array<sup>18,19</sup>.

After preparing the animal as in Fig. 1, changes in RH414 fluorescence were monitored by acquiring pairs of 16-frame (33 ms frame $^{-1}$ ) sequences. Each experimental run consisted of subtracting a 16-frame sequence without the stimulus, from a